

MICRO- AND NANO-FABRICATION USING BESSEL-BEAM ACTIVATED PHOTOPOLYMERIZATION

0339_0501_000088

He Cheng¹, Chun Xia¹, Mingman Sun², Meng Zhang², Stephen M. Kuebler^{1,3}, and Xiaoming Yu^{1*}

¹CREOL, The College of Optics and Photonics, University of Central Florida, Orlando, Florida 32816, USA

²Department of Industrial and Manufacturing Systems Engineering, Kansas State University, Manhattan, Kansas 66506, USA

³Department of Chemistry, University of Central Florida, Orlando, Florida 32816, USA

*yux@creol.ucf.edu

Abstract

Microfabrication based on photopolymerization is typically achieved by scanning a focal spot within the material point-by-point, which significantly limits fabrication speed. In our previous study, we explored a method for rapid fabrication of high-aspect-ratio micro- and nanostructures by scanning the Bessel beam in the plane transverse to the direction of beam propagation. However, the structure fabricated by this method suffers from surface texture. In this work, the origin of these effects is investigated by in-situ measurement of the photopolymerization process. By scanning the laser beam at a speed faster than the polymerization takes place at any given position, we show that it is possible to eliminate the surface texture and obtain smooth surface finish.

Introduction

Multi-photon lithography (MPL) based on photopolymerization has been widely used in microfabrication with sub-micron precision [1,2]. In a classic MPL setup, a femtosecond laser beam is focused into a Gaussian focal spot which is then used to fabricate structures by point-by-point scanning [3]. However, scanning point by point is often time-consuming for fabricating large parts. Various methods have been proposed to speed up fabrication speed, including multi-focus scanning [4] and shell fabrication [5]. Recently, another method that utilizes Bessel beam has been explored [6,7]. Bessel beam generated by axicon has been used to fabricate polymer fibers [7,8]. Modulated Bessel beam generated with a spatial light modulator (SLM) has been used to fabricate micro-tubes [9,10]. In our previous study, we found that the polymer structure

created by Bessel-beam scanning has different types of surface texture [11]. The origin of this phenomenon needs to be identified in order to fabricate parts with smooth surface finish. In this paper, we first investigate the mechanism of the formation of the surface texture. Then, we demonstrate a solution that is based on polymerization kinetics. This work shows the potential of Bessel-beam activated photopolymerization for rapid fabrication of large-scale high-aspect-ratio micro- and nano-structures with good quality for applications in photonics, micro-machines, and tissue engineering.

Experimental setup

The experimental setup is shown in Fig. 1. The laser source was a femtosecond laser (Pharos, Light Conversion) that generated pulses with a full-width-at-half-maximum (FWHM) duration of 170 fs, a center wavelength of 1030 nm, and a repetition rate of 100 kHz. The beam was linearly polarized parallel to the optical table (y axis in Fig. 1(a)). The laser beam was passed through a second-harmonic-generation (SHG) module consisting of a half-wave plate (HWP), a β -barium borate (BBO) crystal and a polarizing beam splitter (PBS). The laser beam was thus converted to the SHG (515 nm) beam and the fundamental (1030 nm) beam was filtered out by PBS. The laser frequency was doubled because we found out in our previous work that 515 nm has a wider power range for fabricating good structures. In the sample cell, an adhesion layer of FormLabs photopolymer (FLGPCL02) was first applied to a single microscope slide, and then a droplet of resin ("Resin base", 3D Ink) was placed onto the surface. Two ways of in-situ monitoring the polymerization process were

implemented – top view (depicted in Fig. 1(a)) and side view (not shown). For the side-view monitoring, a cover slide is attached perpendicularly to the microscope slide edge to create a transparent window, and the fabrication took place near this edge. The sample cells were mounted on a motorized translation stage (Newport ILS100CC) and positioned within the Bessel beam's depth of focus. A camera (Mightex SME-B050-U) was mounted from the side of the

sample for the side-view monitoring. A red light-emitting diode (LED) was used to illuminate the sample for imaging. A long-pass filter was placed in front of the camera to filter out the SHG (515 nm) beam and let the LED light pass through. During the fabrication, the sample was translated in the x-y plan under computer control to synchronize exposure from the Bessel beam. After exposure, the cells were rinsed with isopropyl alcohol (IPA) to remove uncured resin.

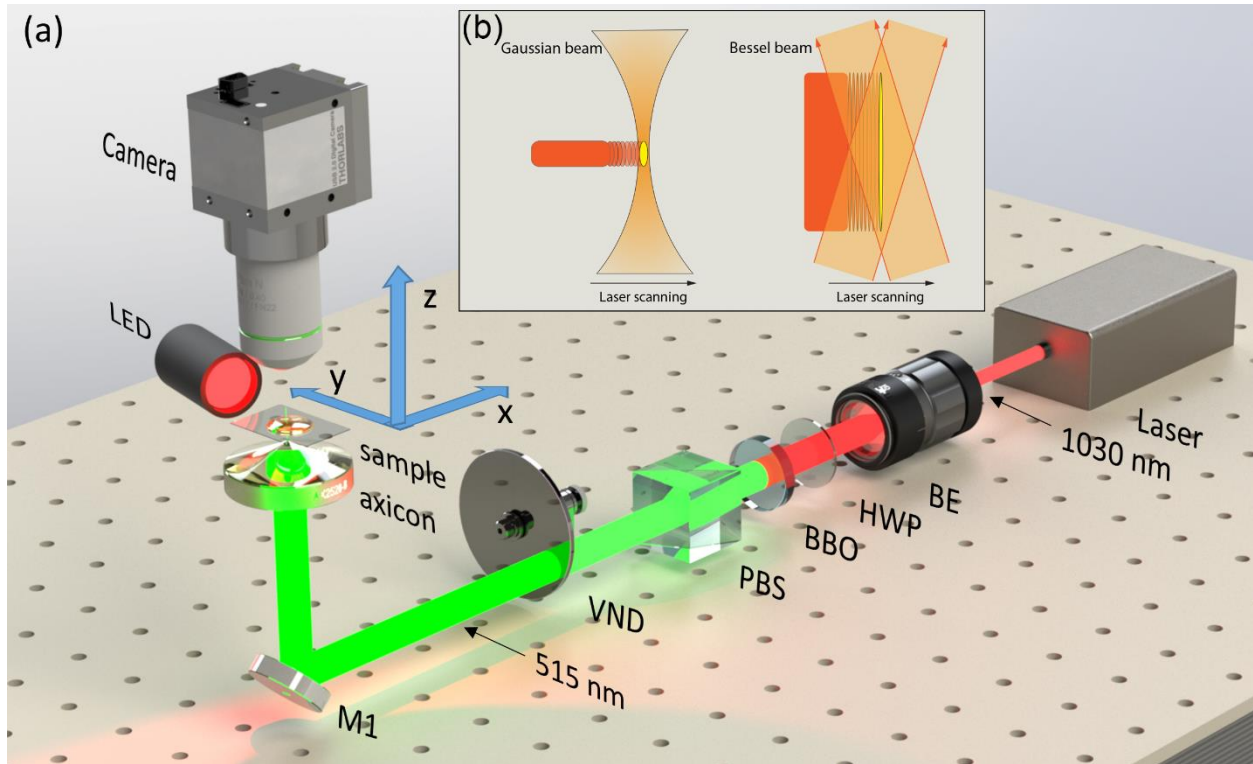


Figure 1 (a) Experimental setup. BE, beam expander; HWP, half-wave plate; BBO, β -barium borate crystal; PBS, polarizing beam splitter; VND, variable neutral density filter; M, mirror; (b) Schematic of beam geometry for the Gaussian beam (left) and the Bessel beam (right). Adapted from Ref. [11].

Results and Discussion

Types of textures

Figure 1(b) shows a comparison of photopolymerization between a Gaussian beam and a Bessel beam. For a Gaussian beam, which is typically used in MPL, the polymerization volume is a tiny focal voxel. When fabricating the structure, the voxel is scanned point by point. The polymer structure formed by previous voxels will not affect the writing beam. When writing with a Bessel beam, in contrast, the voxel is a long narrow needle. By scanning the Bessel beam across the resin, it will generate a polymer sheet. However, due to the shape of the Bessel-beam voxel,

previously formed structure will affect part of the writing beam. The surface of the polymer sheet is therefore not as smooth as what one would expect for a scanned “needle beam”. Figure 2(a-e) are SEM images of polymer structure fabricated by the Bessel beam under various writing condition. Figure 2(a) shows the details of a polymer fiber that is attached to the glass substrate. It was fabricated by stationary exposure with high exposure dose (high power, long exposure time). It is obvious that the shape of the fiber is not a reproduction of the Bessel beam's voxel shape, which is a long needle. The structure appears to consist of many filaments whose diameters range from 1 to 3 μm . Figures 2(b-f) show various types of textures when scanning the Bessel beam in the direction

indicated by the white arrows. These textures can be divided into two groups. One group is periodic textures that are parallel to the optic axis (beam propagation direction). The periodicity is found to range from 1 μm to a few μm . In Figure 2(c) the periodicity is approximately 1 μm . The other one group is the texture inclined at an approximate 10° to

the optic axis. In some cases, e.g., in Figure 2(f), both groups of textures were observed.

Imaging the dynamic polymerization process

To explore the origin of the texture formation, in-situ observation of the photopolymerization process was

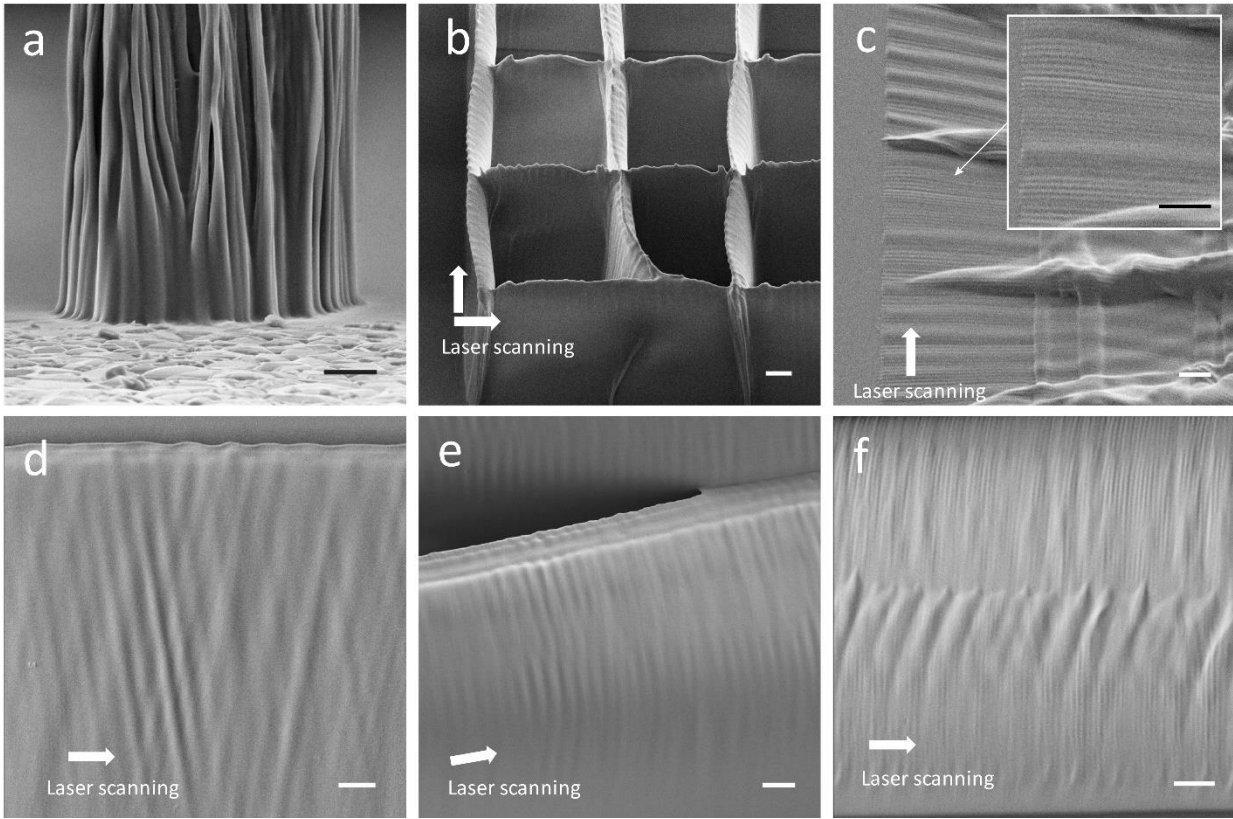


Figure 2 SEM images showing different types of texture at various writing condition. (a) “Filaments” formed under stationary exposure with high exposure dose. (b)(c): Mesh structures formed by scanning the laser beam. Nearly periodic surface texture observed. Scanning speed 0.15 and 0.35mm/s, respectively. (d)(e)(f): Sheet structures fabricated by scanning the Bessel beam at 0.5, 0.2 and 0.05 mm/s, respectively. Different types of filaments and textures observed. White arrows indicate the scanning direction. All scale bars are 10 μm .

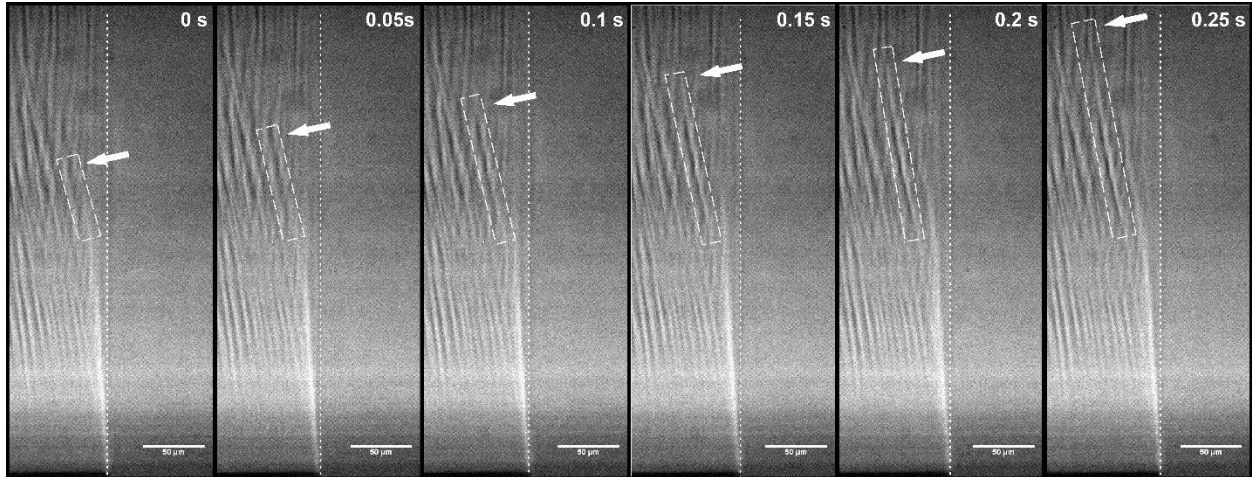


Figure 3 A sequence of transmissive microscopic images show the in-situ measurement of polymerization process of the self-writing filaments. The Bessel beam with average power of 60mW incidents from bottom and scans from left to right at 0.05mm/s. White dash line box shows one growing filament and white arrow points out the front end of the filament in each frame. White dot line shows the axis of the Bessel beam. Contrast of the images was adjusted for better visibility. Scale bars are 50 μm .

made by placing a video camera along the y -axis (see Figure 1(a)) and record a sequence of “side-view” images. The result is shown in Figure 3. The Bessel beam was scanned from left to right. Inclined filaments that appear in Figure 2(d) can be observed (the white dashed box tracks the “growth” of a particular filament). The angle between the filaments’ elongation direction and the Bessel beam axial direction matches the one found in the SEM images shown in Figure 2. The inclined filaments were formed on the left of the laser beam (vertical dashed line) indicating that there is a delay in the formation of the filament. The filament tracked by the white dashed box can be seen to form from the bottom to the top. The filament grows a length of 50 μm in 0.25 s, yielding a speed of 400 $\mu\text{m/s}$. The filaments continue to grow and serves itself as an optical waveguide on the left of the Bessel beam center core (vertical dashed line) where the Bessel beam reaches its maximum intensity. These observations lead us to believe that this phenomenon is related to the self-writing effect in photopolymerizable material [8,12]. We believe that part of the beam was guided into and trapped inside the polymer sheet and cause self-writing of polymerized filaments.

We also notice that there are filaments formed right at the center of Bessel beam. These filaments correspond to those found in the SEM images that are parallel to the beam axial direction. Since the formation speed is

much faster than those self-written filaments, we suspect that there are other mechanisms involved in the formation of complex surface texture, such as the one shown in Figure 2(f). As mentioned above, there is a fundamental difference of the writing beam geometry between the Gaussian and Bessel beam, for the latter of which the beam profile will be influenced by the previously formed structure. This “self-modulation” effect on the writing beam intensity profile may result in the filaments as well.

Estimation of polymerization time

A previous study shows that commercial acrylate photopolymer exhibits an intrinsic polymerization duration τ , which is the time between the exposure and the settlement of polymerization, under very short exposure [13]. During this process, the refractive index will gradually increase as the monomer cross-links. This gives us a means to eliminate the formation of surface texture/filaments. First, if the laser beam scanning speed is increased until at a certain value that the polymer structure forms behind the beam center far enough, the polymer sheet will not influence the writing beam. Second, by increasing the scanning speed, the light that is self-trapped inside the polymer sheet will not have enough time to finish the self-writing process. We performed the experiment shown in Figure 4 to measure the intrinsic polymerization time of our photopolymer. It is based on the fact the polymer structure formation leads to change in refractive index and hence a change in the

transmission of the image (contrast of the polymerized structure). Here the camera was mounted as shown in the Figure 1(a), and the sample cell was translated in the x-y plane. Several images under different scanning speed were captured (one example is shown in Figure 4(a)). It can be clearly observed that the contrast of the image gradually changes as the distance to the center of the beam increases. The distance, when divided by the scanning speed, translates to the time after laser exposure. The refractive index change is assumed to be proportional to the polymerization conversion rate so that the edge contrast extract from image can be associated with the progress of the polymerization reaction [13]. Although the polymer sheet image in Figure 4(a) looks like a blurred image due to movement of the object, it should be noticed that it will not be blurred despite the camera exposure time since the polymer sheet grew from the beam center. Using this method, we find that the typical time constant $\tau = 1.1 \pm 0.2$ ms.

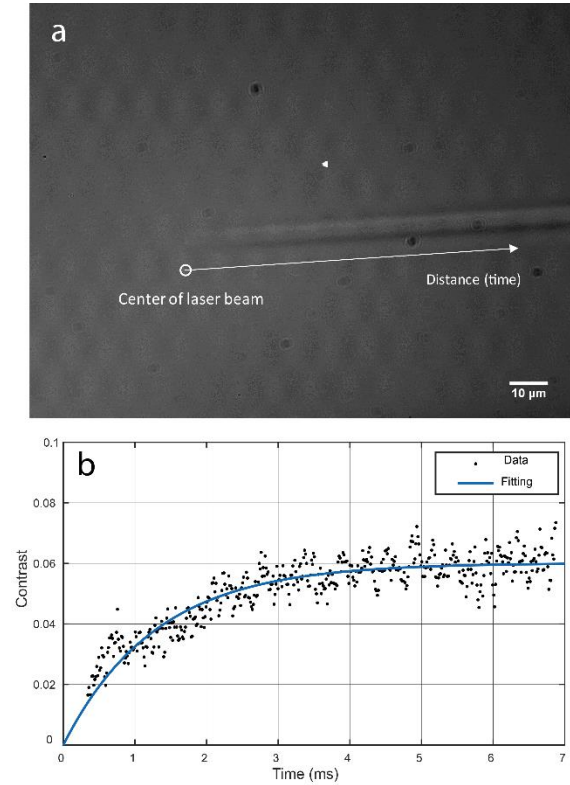


Figure 4 (a) A transmissive microscopic image was taken while the structure is under photopolymerization. The stage is moving while the position of the camera and the laser is relatively stationary. Scanning speed was 8 mm/s. (b) The contrast of the forming structure is extract from the image to estimate the polymerization time. The intrinsic polymerization time is determined by fitting

the data with a function $S_{contrast} = S_0(1 - e^{-t/\tau})$, where S_0 and τ are fitting parameters.

Base on the simple geometry of the Bessel beam shown in Figure 1 (b), for structure with 100 μm height, the influence of the polymer structure on the writing beam can be eliminated when the scanning speed exceeds 15 mm/s. In practice, we find that with a scanning speed of 4 mm/s, the surface texture is not visible under SEM (Figure 4). This is due to the estimation of 15 mm/s based on the two-dimension geometry in Figure 1 is an overestimation. A slower speed is required in three-dimensional geometry since the polymer sheet will only affect a fraction of the Bessel beam.

Comparison to Gaussian beam

To better understand the mechanism of the filamentation and surface texture generation, we used a small NA lens to generate a Gaussian beam with long depth of field (DOF) of 1 mm and 13 μm beam waist and repeated the experiment. Figure 6 (a) shows the transmissive microscope images that were taken during photopolymerization. We again observed the similar phenomenon occurred in the previous experiment using the Bessel beam. The self-writing filament can be more clearly recognize and each filament extends out and eventually became individual fibers. The similarity between these two experiments indicates the filamentation does not originate from the beam profile. It is hypothesized that this is related to the modulation instability seeded by noise in photopolymerizable material [14]. Figure 6 (b)(c) shows the polymer sheet before and after development. Due to this self-writing mechanism, fabrication of a high-aspect-ratio structure with good quality cannot be achieved easily by Gaussian beam. For Bessel-beam activated polymerization, due to its non-diffraction property, high-aspect-ratio polymer sheets were fabricated more easily and had sharper and smother top edge.

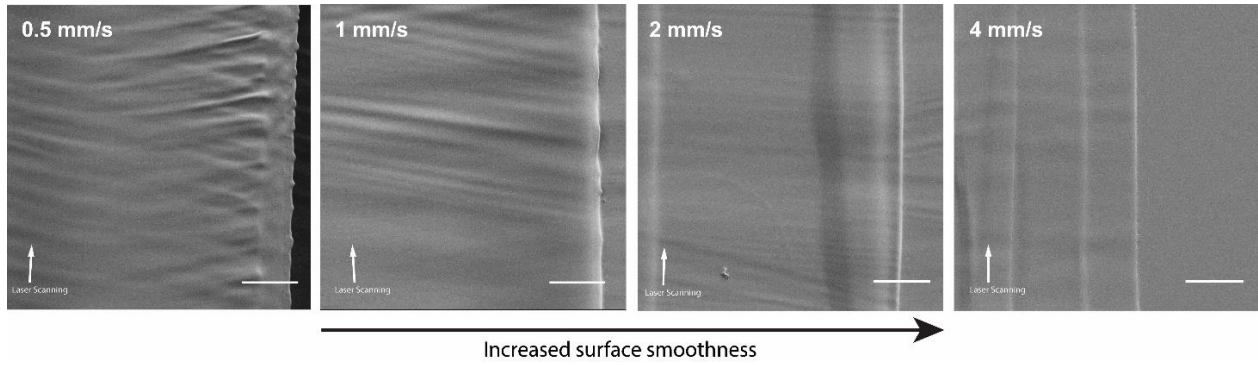


Figure 5 SEM images of polymer sheets fabricated with laser scanning speed of 0.5, 1, 2 and 4 mm/s, respectively. Increasing scanning speed produces smoother surface. Scale bars are 20 μm .

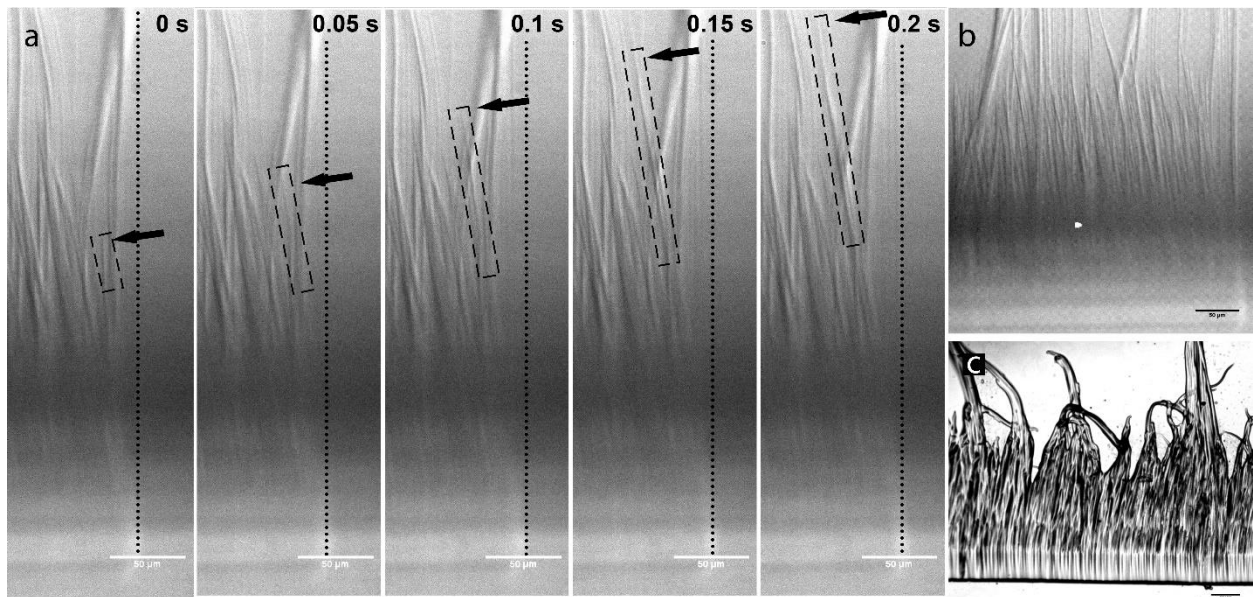


Figure 6 (a) A sequence of transmissive microscopic images showing the in-situ observation of photopolymerization and the self-writing filaments with a Gaussian beam. A Gaussian beam with $\sim 1\text{ mm}$ DOF (depth of field) enters from the bottom and scans from the left at 0.05 mm/s. The axis of Gaussian beam is shown by the black dot lines. Black dash line box tracks the formation of one filament, and the black arrows point out the front end of the filament in each frame. (b) A microscopic image of the structure before development. (c) A microscopic image of developed structure shows that Gaussian beams are not suitable for producing high-aspect-ratio structure. Scale bars are 50 μm .

Conclusion

In-situ monitoring of the photopolymerization process by transmissive microscopic imaging reveals the self-writing mechanism in Bessel-beam activated photopolymerization. It is found that the photopolymerization intrinsic duration for the photopolymer used in this study is 1.1 ms, which is long enough to eliminate the filamentation by simply increasing the scanning speed. The result from repeating the experiment with a long depth-of-focus Gaussian beam provides evidence of the self-writing theory and shows the advantage of using Bessel beam

to fabricate high-aspect-ratio structures. However, the formation mechanism for parallel filamentations with a periodicity on the order of 1 μm is yet to be found and further study is needed. We have addressed the fundamental issues in photopolymerization by scanning Bessel beam and provided a simple solution to generate parts with smooth surface finish. This shows the potential of this method for rapid fabrication of large-scale high-aspect-ratio micro- and nano-structures with good quality for applications in photonics, micro-machines, and tissue engineering.

Reference

1. S. Kawata, H. B. Sun, T. Tanaka, and K. Takada, "Finer features for functional microdevices," *Nature* **412**(6848), 697–698 (2001).
2. S. H. Park, D. Y. Yang, and K. S. Lee, "Two-photon stereolithography for realizing ultraprecise three-dimensional nano/microdevices," *Laser Photonics Rev.* **3**(1–2), 1–11 (2009).
3. M. Farsari and B. N. Chichkov, "Materials processing: Two-photon fabrication," *Nat. Photonics* **3**(8), 450–452 (2009).
4. G. Vizsnyiczai, L. Kelemen, and P. Ormos, "Holographic multi-focus 3D two-photon polymerization with real-time calculated holograms," *Opt. Express* **22**(20), 24217 (2014).
5. D. Wu, Q. D. Chen, L. G. Niu, J. N. Wang, J. Wang, R. Wang, H. Xia, and H. B. Sun, "Femtosecond laser rapid prototyping of nanoshells and suspending components towards microfluidic devices," *Lab Chip* **9**(16), 2391–2394 (2009).
6. X. F. Li, R. J. Winfield, S. O'Brien, and G. M. Crean, "Application of Bessel beams to 2D microfabrication," *Appl. Surf. Sci.* **255**(10), 5146–5149 (2009).
7. X. Yu, M. Zhang, and S. Lei, "Multiphoton Polymerization Using Femtosecond Bessel Beam for Layerless Three-Dimensional Printing," *J. Micro Nano-Manufacturing* **6**(1), 010901 (2017).
8. J. Jezek, T. Cizmár, V. Nedela, and P. Zemánek, "Formation of long and thin polymer fiber using nondiffracting beam.," *Opt. Express* **14**(19), 8506–8515 (2006).
9. L. Yang, S. Ji, K. Xie, W. Du, B. Liu, J. L. Yanlei Hu, G. Zhao, D. Wu, W. Huang, S. Liu, H. Jiang, and J. Chu, "High efficiency fabrication of complex microtube arrays by scanning focused femtosecond laser Bessel beam for trapping / releasing biological cells," *Opt. Express* **25**(7), 3167–3178 (2017).
10. S. Ji, L. Yang, C. Zhang, Z. Cai, Y. Hu, J. Li, D. Wu, and J. Chu, "High-aspect-ratio microtubes with variable diameter and uniform wall thickness by compressing Bessel hologram phase depth," *Opt. Lett.* **43**(15), 3514 (2018).
11. H. Cheng, C. Xia, M. Zhang, S. M. Kuebler, and X. Yu, "Fabrication of high-aspect-ratio structures using Bessel-beam-activated photopolymerization," *Appl. Opt.* **58**(13), D91 (2019).
12. A. S. Kewitsch and A. Yariv, "Self-focusing and self-trapping of optical beams upon photopolymerization.," *Opt. Lett.* **21**(1), 24–6 (1996).
13. J. B. Mueller, J. Fischer, F. Mayer, M. Kadic, and M. Wegener, "Polymerization Kinetics in Three-Dimensional Direct Laser Writing," *Adv. Mater.* **26**(38), 6566–6571 (2014).
14. L. Qiu and K. Saravanamuttu, "Modulation instability of incandescent light in a photopolymer doped with Ag nanoparticles," *J. Opt. (United Kingdom)* **14**(12), (2012).